Biochemical and Biophysical Research Communications 503 (2018) 2736–2741

Contents lists available at ScienceDirect

Biochemical and Biophysical Research Communications

journal homepage: www.elsevier.com/locate/ybbrc

# Structural motifs in the RGS RZ subfamily combine to attenuate interactions with Gα subunits

Denise Salem-Mansour, Ali Asli, Meirav Avital-Shacham, Mickey Kosloff*

*The Department of Human Biology, Faculty of Natural Science, University of Haifa, Haifa, 3498838, Israel*

ARTICLE INFO

*Article history:*
Received 25 July 2018
Accepted 3 August 2018
Available online 13 August 2018

*Keywords:*
G protein signaling
RGS proteins
GTPase
Interaction specificity
PPI
Protein structure

ABSTRACT

Regulators of G-protein Signaling (RGS) proteins inactivate heterotrimeric G proteins, thereby setting the duration of active signaling. In particular, the RGS RZ subfamily, which consists of RGS17, RGS19, and RGS20, mediates numerous physiological functions and human pathologies – mostly by functioning as GTPase Activating Proteins (GAPs) towards the $G\alpha_i$ subfamily. Yet, which RZ subfamily members mediate particular functions and how their GAP activity and specificity are governed at the amino acid level is not well understood. Here, we show that all RZ subfamily members have similar and relatively low GAP activity towards $G\alpha_o$. We characterized four RZ-specific structural motifs that mediate this low activity, and suggest they perturb optimal interactions with the Gα subunit. Indeed, inserting these RZ-specific motifs into the representative high-activity RGS16 impaired GAP activity in a non-additive manner. Our results provide residue-level insights into the specificity determinants of the RZ subfamily, and enable to study their interactions in signaling cascades by using redesigned mutants such as those presented in this work.



## 1. Introduction

Heterotrimeric (αβγ) G proteins function as ubiquitous molecular switches in signal transduction pathways. Activated Gα subunits are turned "off" by Regulators of G-protein Signaling (RGS) proteins, which mediate numerous physiological functions and human pathologies [1–4], and are therefore considered promising therapeutic targets [5–7]. RGS proteins inactivate Gα subunits by allosterically accelerating their intrinsic GTPase activity. In particular, the ~120 residue "RGS domain", which is present in all RGS proteins, underlies their function as GTPase Activating Proteins (GAPs) [1]. A notable RGS subfamily is the RZ subfamily, whose members RGS17, RGS19, and RGS20 were identified as GAPs for the $G\alpha_i$ subfamily [8–11]. This subfamily has been implicated in central processes such as cell proliferation, neuronal regulation, and tumorigenesis [12–15]. However, which RZ subfamily members mediate particular signaling cascades and what are the molecular determinants of their specific interactions with Gα subunits are not well understood.

Previous reports of the RZ subfamily GAP activity towards members of the $G\alpha_i$ subfamily vary [11]. Earlier studies showed that RGS20 is selective for $G\alpha_z$ and suggested it has minimal GAP activity towards other $G\alpha_i$ subfamily members such as $G\alpha_{i2}$ and $G\alpha_o$ [16,17]. In contrast, Wang et al. showed that RGS19 and RGS20 had similarly high GAP activity towards $G\alpha_{i1}$ as compared to RGS4 [18], a representative high-activity RGS from the R4 subfamily [19]. On the other hand, Mao et al. measured higher GAP activities of RGS17 than RGS20 towards various members of the $G\alpha_i$ subfamily, while both RZ subfamily members had lower GAP activities than RGS4 [10]. More recently, RGS17 was shown to exhibit low GAP activity towards $G\alpha_o$, compared to the high-activity RGS4 and RGS16 [20]. It is therefore unclear what is the relative GAP activity of each RZ subfamily member, and how these activities are governed at the amino acid level.

In previous studies, we classified RGS residues that determine interactions with Gα subunits into three groups, based on their mechanistic role in interactions with Gα subunits. The first group, "Significant & Conserved" (S&C) residues, contains residues that contribute favorably and similarly to interactions with Gα subunits across all high-activity RGS domains [20,21]. The second group, "Modulatory" residues, contains residues that contribute to interactions with Gα subunits only in some high-activity RGS domains and were proposed to fine-tune G protein recognition [20]. The third group, "Disruptor" residues, was recently identified in the

* Corresponding author. Department of Human Biology, Faculty of Natural Sciences, University of Haifa, 199 Aba Khoushy Ave., Mt. Carmel, Haifa, 3498838, Israel.
*E-mail address:* kosloff@sci.haifa.ac.il (M. Kosloff).

https://doi.org/10.1016/j.bbrc.2018.08.033
0006-291X/

RGS R12 subfamily and shown to function as negative design elements; namely these residues attenuate RGS activity for particular Gα subunits by reducing GAP activity in a specific fashion [21]. With regard to RGS17, previous work identified seven residues that determine its interaction with $G\alpha_o$, and showed that substitution of all seven residues led to a gain of function, increasing the activity of RGS17 to that of the high-activity RGS16 [20]. However, the mechanistic role of these putative RGS17 "specificity-determining" residues was not investigated, nor how they combine to modulate specific interactions with Gα subunits.

Here, we characterized the structural role of the seven specificity-determining residues of RGS17 and compared RGS17 to RGS19 and RGS20. We found that all three RZ subfamily members have similar activity towards $G\alpha_o$, governed by these seven "RZ-specificity determining" residues. We characterized these structural motifs using structure-based modeling, suggesting they attenuate interactions with Gα subunits by a combined interaction with residues from both the Gα GTPase and helical domains. Indeed, insertion of these RZ-specificity determining residues into the high-activity RGS16 substantially reduced RGS GAP activity. This residue-level understanding of the functional specificity determinants of the RGS RZ subfamily can guide the development of RGS-directed therapeutics aimed at this subfamily.

## 2. Materials and methods

### 2.1. Protein structures and sequences

We used the following 3D structures in our analysis and visualization of Gα-RGS complexes (with PDB codes for each structure): $G\alpha_{i1}$—human RGS16 (2IK8) and RGS17 (1ZV4) [22]. Missing residues in 2IK8 ($G\alpha_{i1}$ residues 112–118) and 1ZV4 (S145) were predicted using Nest [23], and partial or missing side chains in 1ZV4 (L144, R184) were predicted using Scap [24].

### 2.2. Protein expression, purification, and activity analysis

RGS19 and RGS20 were obtained from the cDNA Resource Center (www.cdna.org), while RGS16 and RGS17 were obtained from Addgene. Rat $G\alpha_o$ was a gift from Vadim Arshavsky (Duke University). All RGS domains were expressed in the pLIC-SGC1 vector (Addgene). All proteins were expressed as N-terminally $His_6$-tagged fusion proteins and purified from transformed *Escherichia coli* BL-21 (DE3) cells as described previously [21]. Dose-response analyses of RGS GAP activity were performed as in Ref. [21], using 500 nM $G\alpha_o$ pre-loaded with 1 μM [$\gamma$-$^{32}$P]-GTP and RGS domains in concentrations ranging from 0.5 nM to 3 μM at 4 °C.

## 3. Results

### 3.1. RZ subfamily members show lower GAP activity towards $G\alpha_o$ than the high-activity RGS16

We measured the GAP activities of the three RZ subfamily members (RGS17, RGS19, and RGS20) towards the representative $G\alpha_i$ subfamily member $G\alpha_o$, and compared it to that of RGS16, a representative R4 high-activity RGS domain [20,21]. We used dose response analysis to quantify and compare the GAP activity of these RGS domains, as this analysis provides a more accurate measurement of RGS activity [21]. This comparison showed that all three RZ family members have similarly low GAP activities compared to RGS16. As expected from previous studies [20], replacing all seven RGS17 specificity-determining residues with their corresponding RGS16 residues (the RGS17 > 16 mutant) increased the GAP activity of this mutant to that of RGS16, confirming that these seven residues are sufficient to determine the lower GAP activity of RGS17.

### 3.2. The RZ subfamily contains four structural motifs that are conserved across this subfamily but diverge from high-activity RGS domains

To characterize the functional role of the seven RGS17 specificity-determining positions, we compared these amino acid positions in the RZ subfamily and across representative high-activity members from the R4 subfamily (Fig. 2). We found that all seven residues are essentially conserved across all RZ subfamily members, and can be assigned into four distinct motifs (Fig. 2A). Three of these (the "ILS", "S*", and "HR" motifs) are identical across all three RZ members, while the "N" motif, which is an asparagine in RGS17 and RGS20, is a serine in RGS19 (Fig. 2A). As shown previously [20,21], residues in the high-activity R4 RGS domains that correspond to these four motifs contribute favorably to the interactions of these RGS domains with $G\alpha_i$ and $G\alpha_o$ (Fig. 2B). Supporting the functional importance of these positions, mutations in R4 residues located in these four motifs were shown to impair GAP activity [20,21,25–27]. Two of these positions (RGS16 A126 and N131) were previously classified as S&C residues that contribute to interactions with Gα subunits in all high-activity RGSs, while four positions were classified as Modulatory residues that are usually non-conserved and can contribute to interactions with Gα subunits only in some RGS domains (Fig. 2B) [20,21]. Moreover, the HR motif in the RZ subfamily corresponds to a Disruptor motif that was identified in the R12 RGS subfamily; a lysine-tyrosine or a lysine-phenylalanine motif in the corresponding positions in the R12 subfamily members RGS10 and RGS14 led to significantly impaired GAP activity [21].

We modeled the RGS17-$G\alpha_i$ complex by superimposing the RGS17 monomer, as a structural representative of the RZ subfamily, onto the RGS16 coordinates in the RGS16-$G\alpha_i$ complex. We see that the four RZ-specific motifs are spaced along the RGS domains with no apparent intramolecular interactions between them (Fig. 2C). The ILS and S* motifs interact only with the Gα GTPase domains, with the former in the periphery of the interface, and the latter

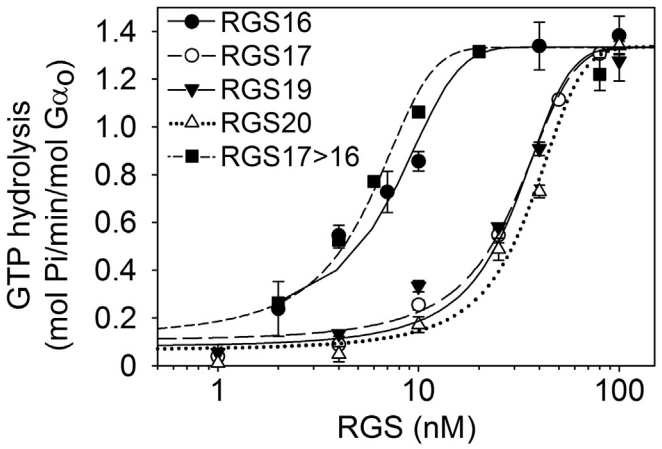


**Fig. 1.** RGS RZ subfamily members RGS17, 19, and 20 show similarly low GAP activity towards $G\alpha_o$, compared to the high-activity RGS16. Dose-response analysis of the GAP activity of the following RGS domains toward $G\alpha_o$: RGS16, RGS17, RGS19, RGS20, and the RGS17 > 16 mutant (where all seven previously-identified RGS17 specificity-determining residues were substituted with the corresponding RGS16 residues: I143S + L144E + S145A + S150N + H183E + R184K + N192K). $EC_{50}$ values are: RGS16 = 7 ± 1 nM, RGS17 = 30 ± 2 nM, RGS19 = 29 ± 3 nM, RGS20 = 36 ± 2 nM, RGS17 > 16 = 5 ± 1 nM, and were calculated using three-parameter sigmoidal curves in SigmaPlot 10.0. Data are means ± SEM of experiments performed in triplicate, representative of three or more independent biological replicates for each RGS.

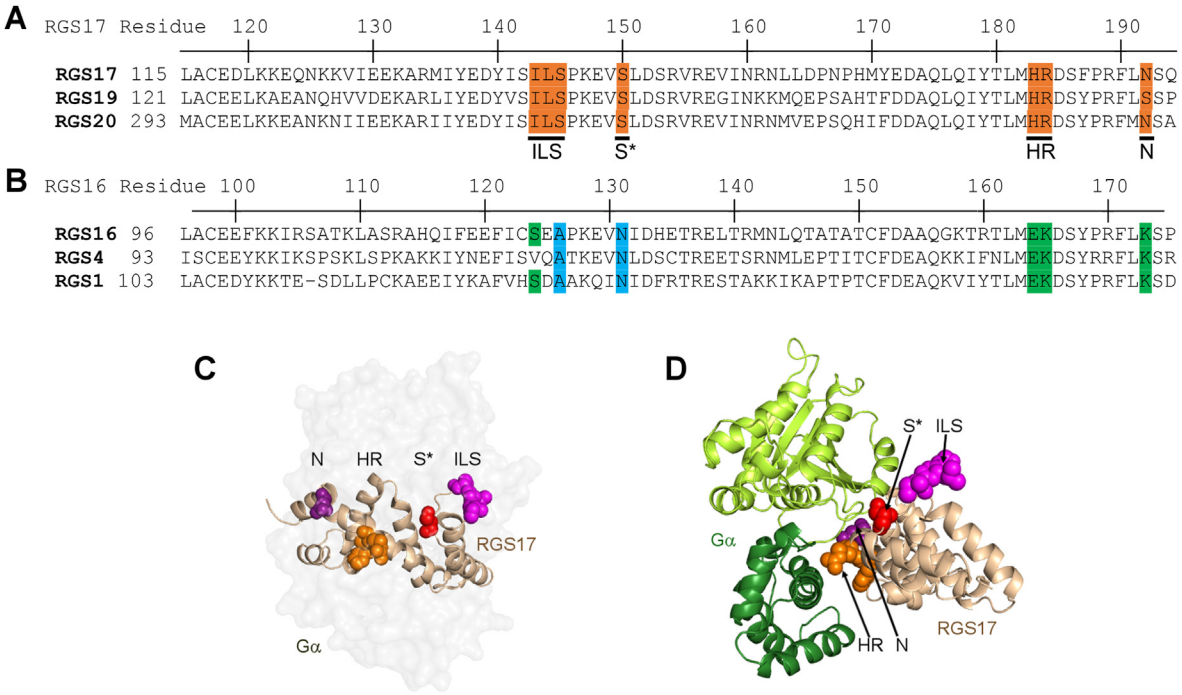





**Fig. 2.** Comparison of RGS RZ specificity-determining residues and the corresponding residues in high-activity R4 RGS domains. (A) Sequence alignment of the three human RZ subfamily domains (with UNIPROT IDs): RGS17 (Q9UGC6), RGS19 (P49795), RGS20 (O76081). The seven specificity-determining residues identified in RGS17 (marked in orange) were assigned to four distinct motifs that are marked below the alignment. (B) Sequence alignment of three representative R4 high-activity RGS domains (with UNIPROT IDs): RGS16 (O15492), RGS4 (P49798), RGS1 (Q08116). Conserved S&C residues, shown previously to contribute to interactions with Gα subunits in all R4 high-activity RGS domains, are marked in blue. Modulatory residues, which are usually non-conserved and can contribute to interactions with Gα subunits only in some RGS domains, are marked in green. (C) Model of the RGS17-$G\alpha_i$ complex. The RGS17 monomer (PDB ID 1ZV4) was superimposed onto the RGS16 coordinates in the RGS16-$G\alpha_i$ complex x-ray structure (PDB ID 2IK8), shown as a ribbon diagram and viewed through the transparent surface of the Gα subunit. The ILS, S*, HR, and N motifs that are marked in A are shown as spheres, with a different color for each motif. (D) Putative interactions of the RZ-specific RGS17 motifs with the Gα subunit. RGS17 is shown as in C, rotated 90° about the y-axis. $G\alpha_{i1}$ is shown as a ribbon diagram, with the GTPase domain colored green and the helical domain colored dark green. (For interpretation of the references to color in this figure legend, the reader is referred to the Web version of this article.)

buried in the middle of the interface (Fig. 2D). On the other hand, the HR and N motifs are closer together and interact with the Gα helical domain (Fig. 2D).

### 3.3. *RZ-specificity determining motifs are predicted to attenuate interactions with Gα subunits*

To investigate the mechanistic basis for how the seven RZ-specificity determining residues attenuate Gα recognition, we compared the interactions of RGS17 with $G\alpha_i$ to those of RGS16, a representative of the high-activity R4 subfamily, with $G\alpha_i$ (Fig. 3). Note that $G\alpha_i$ and $G\alpha_o$ interact similarly with high-activity RGS domains, and that $G\alpha_i$ is better characterized among the available Gα complexes with RGS domains [21]; $G\alpha_i$ is therefore a more reliable choice for such structural comparisons [28].

Analyzing the model of the RGS17-$G\alpha_i$ complex, we see that the RGS17 ILS motif consists of two large hydrophobic residues (RGS17 I143 and L144) and one polar residue (RGS17 S145) (Fig. 3A, upper). These residues cannot form the electrostatic or polar interactions with $G\alpha_i$ R205 and K209 that are formed by the corresponding RGS16 residues (RGS16 S124, E125, and A126; Fig. 3A, lower). Moreover, the absence of coordinates for the side chains of both RGS17 S145 and L144 in the PDB structure suggests the backbone of the ILS motif is especially flexible, and that this flexibility might attenuate interactions with $G\alpha_i$. This hypothesis is supported by analysis of the NMR structure of RGS19, which shows enhanced flexibility in the α5-α6 loop that contains the ILS motif (Supp. Fig. S1) and by B-factor analysis of the monomer x-ray structure of RGS17, which also suggests enhanced flexibility of the same loop (Supp. Fig. S2).

The RGS17 HR motif corresponds to a glutamate-lysine motif in high activity RGS domains that forms an electrostatic and hydrogen bond network with multiple residues on both sides of the interface [21]. As detailed above, the corresponding residues in RGS10 (lysine-tyrosine) and RGS14 (lysine-phenylalanine) were shown to perturb these interactions and attenuate GAP activity [21]. When we compared RGS17 and RGS16, we saw that while RGS17 R184 can potentially interact with $G\alpha_i$ S75 and E116 similarly to the corresponding RGS16 K165, the RGS17 H183 residue cannot substitute for the intra-molecular salt bridge formed by RGS16 E164 (Fig. 3B). This suggests that the RGS17 HR motif may partially perturb interactions with $G\alpha_i$, but less so than the RGS10 and RGS14 Disruptor residues. Notably, the RGS17 HR motif is adjacent to the N motif (N192), and this asparagine residue is too short to interact favorably with $G\alpha_i$ E65 (Fig. 3B). As shown above, RGS19 has a serine in this position, which we predict is also too short to interact favorably with $G\alpha_i$ E65 (not shown). Therefore, despite this difference in amino acids, the N motif of all members of RZ subfamily is predicted to have a similar effect on interactions with the Gα subunit. This analysis also suggests that due to the proximity of the HR and N motifs, their effect on interactions with Gα subunits is not mutually exclusive, and should be regarded as a joint motif, which we call the HR + N motif.

The RGS17 S* motif (S150) stands out in its pivotal location at the center of the interface with $G\alpha_i$ (Fig. 2D) and its multiple interactions with critical Gα residues (Fig. 3C). The RGS16 residue in this position is an asparagine (termed here $Asn_{S\&C}$) that is conserved across all RGS domains except for the RZ subfamily. This

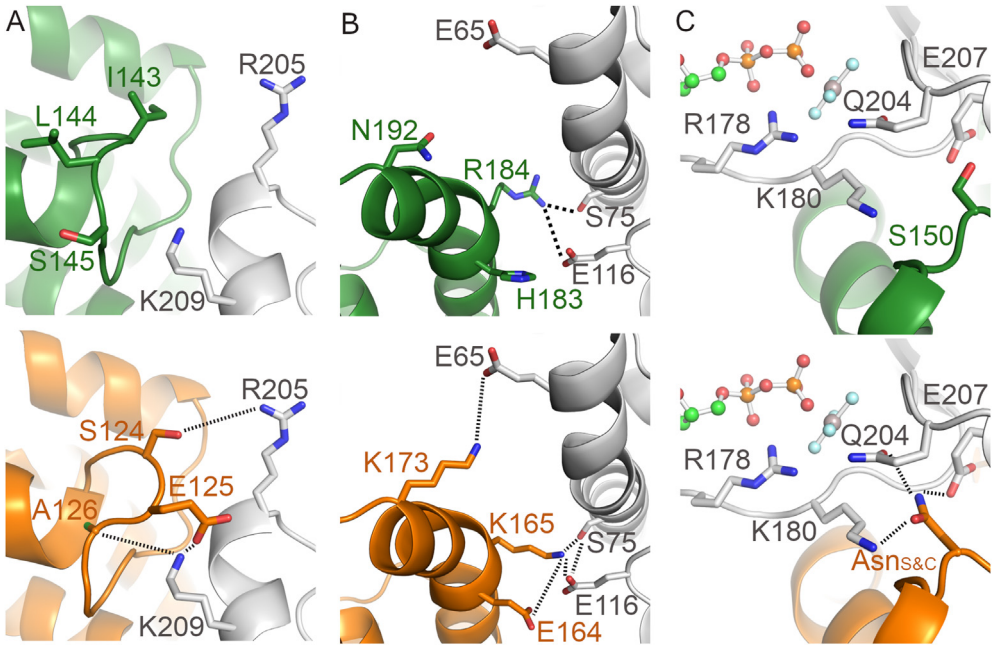


**Fig. 3.** Predicted interactions of the RGS17 specificity-determining motifs with $G\alpha_i$, compared to the corresponding interactions in RGS16 bound to $G\alpha_i$. The RGS17-$G\alpha_i$ complex was modeled as in Fig. 2. RGS17 (colored green, upper panels), RGS16 (colored orange, lower panels), and the $G\alpha$ subunit (colored grey) are shown as ribbon diagrams. Salt bridges or hydrogen-bonds in the crystal structure are marked with dashed lines, while predicted salt bridges between RGS17 and $G\alpha_i$ are marked with dotted lines. (A) The RGS17 ILS motif (I143, L144, and S145, upper) cannot form the favorable interactions of the corresponding RGS16 residues (S124, E125 and A126, lower) with $G\alpha_i$ R205 and K209. (B) The RGS17 HR and N motifs interact with adjacent residues in the $G\alpha$ helical domain. The RGS17 HR motif (H183 and R184) can only partially form the favorable interactions of the corresponding RGS16 E164 and K165 residues, which form a network of intra- and inter-molecular interactions with $G\alpha_i$ S75 and E116 (lower). The RGS17 N motif (N192, upper) cannot form the favorable interaction made by the corresponding RGS16 K173 with $G\alpha_i$ E65 (lower). (C) The RGS17 S* motif cannot form the intricate network of interactions made by the RGS16 $Asn_{S\&C}$ residue with $G\alpha_i$ E207, the catalytic residue Q204, and K180 (lower). The $G\alpha_i$ catalytic residue R178 is also shown, as the nearby K180 likely affects its orientation. The guanine nucleotide (from PDB ID 2IK8) is shown in ball and stick representation, colored by element. (For interpretation of the references to color in this figure legend, the reader is referred to the Web version of this article.)

asparagine forms an intricate network of interactions with several noteworthy $G\alpha_i$ residues: K180, Q204, and E207 (Fig. 3C, lower). Q204 is a catalytic residue that is directly involved in GTP hydrolysis, E207 is adjacent to this residue, and K180 is adjacent to the second $G\alpha$ catalytic residue, R178 [29]. The RZ subfamily serine in the S* motif cannot form these interactions and is therefore predicted to substantially perturb the ability of the RGS domain to accelerate GTP hydrolysis (Fig. 3C, upper).

### *3.4. Inserting the RZ-specificity determining motifs into the high-activity RGS16 impairs GAP activity*

To examine the mechanistic effect of the RZ-specificity determining motifs characterized above, we inserted them into the high-activity RGS16 and measured the effect using dose response analysis (Fig. 4). Inserting the individual ILS motif into RGS16 had a minor effect on GAP activity (Fig. 4A). The combined HR + N motif had a more substantial effect, increasing the $EC_{50}$ by about two-fold (Fig. 4B). The majority of this effect comes from the HR residues in this combined motif (Fig. 4B). Combining all three motifs together into the RGS16 ILS + HR + N mutant increased the $EC_{50}$ further, from 7 nM (RGS16 wild-type) to 17 nM (Fig. 4C). Surprisingly, when we mutated the RGS16 $Asn_{S\&C}$ to a serine (the RGS16-S* mutant), the GAP activity of this mutant decreased substantially, with an $EC_{50}$ an order of magnitude lower (380 nM) than that of RGS17 (Fig. 4D).

## 4. Discussion

Our results show that compared to the high-activity RGS16, RZ subfamily members RGS17, RGS19, and RGS20 have lower GAP activity towards $G\alpha_o$. We posit that this low activity is the result of four RZ-specific motifs (Fig. 2), which function in an identical way across the RZ subfamily. Substitution of the corresponding residues in RGS16 with the RGS17 ILS, HR and N motifs reduced the GAP activity of RGS16, validating the suggested disruptory nature of these motifs. The disruptory effect of the ILS motif correlates with high flexibility in this region. The HR and N motifs function jointly by partially disrupting a polar/electrostatic network with the helical domain of the $G\alpha$ subunit – a $G\alpha$ domain that was recently shown to play an important role in interactions with other RGS subfamilies [21,28]. The HR and N motifs reduce GAP activity compared to their RGS16 counterparts, but to a lesser extent than the corresponding KY/KF Disruptor motifs that were previously characterized in the R12 subfamily [21]. Furthermore, the combination of the ILS, HR, and N motifs reduced RGS16 GAP activity more substantially than each motif separately. Importantly, substitution of the $Asn_{S\&C}$ residue in RGS16 with the S* motif had a more dramatic effect on GAP activity than all other three motifs combined. This quantitative effect is supported by previous studies that mutated the $Asn_{S\&C}$ residue in RGS4 and RGS16 and showed a substantial impairment of GAP activity towards $G\alpha_o$ and $G\alpha_i$ [25,26,30]. Nevertheless, the GAP activity of wild type RGS17 is higher than the RGS16 N131S mutant (Fig. 4D), suggesting all of the RZ-specificity determining residues combine in a non-additive way to produce this difference in activity.

More generally, because the RGS17 specificity-determining motifs are essentially identical to those of RGS19 and RGS20, we suggest that the four motifs we characterized here function similarly across the entire RZ subfamily. Therefore, these residue-level insights into the specificity determinants of the RZ subfamily enable to study the interactions of individual RZ subfamily

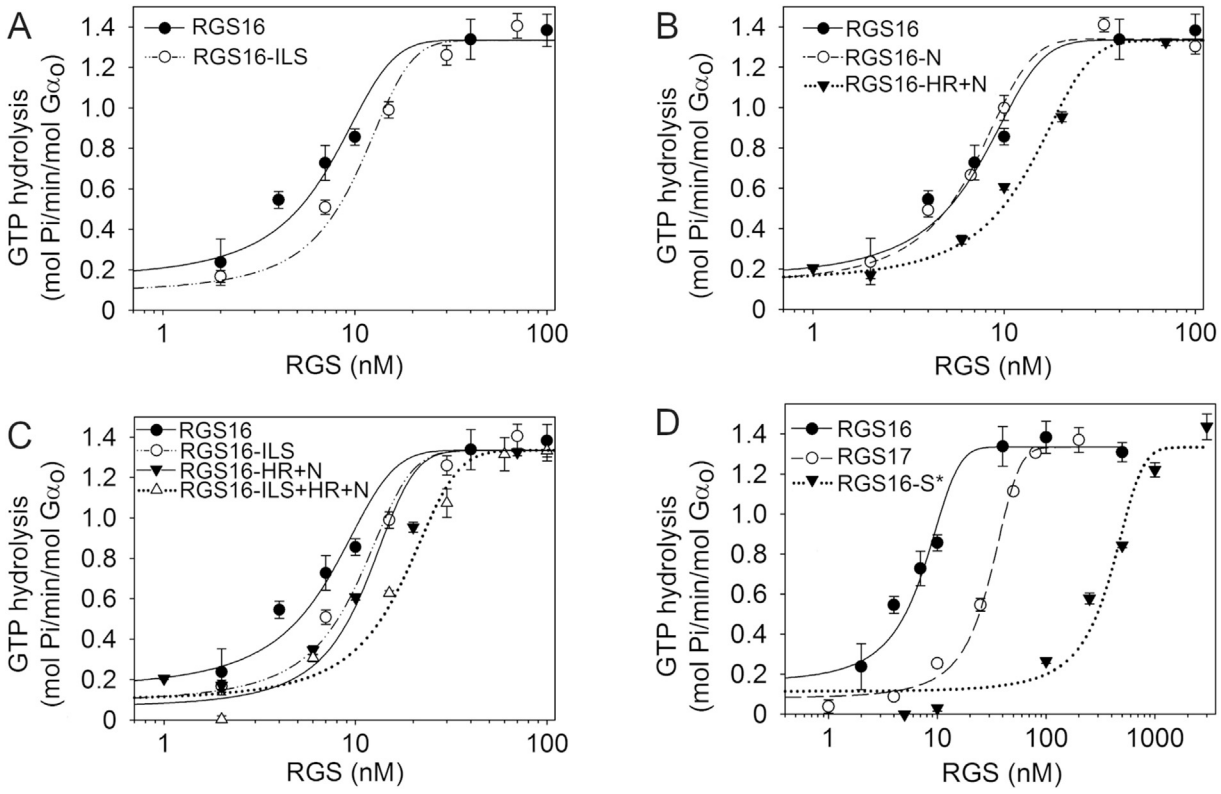


**Fig. 4.** Insertion of the RZ-specificity determining motifs into RGS16 impairs GAP activity. Dose response analysis of the GAP activity of RGS16 and RGS16-to-RGS17 mutants towards $G\alpha_o$. (A) Dose response curves of RGS16 (black circles) and the RGS16-ILS mutant (RGS16 S124I + E125L + A126S). $EC_{50}$ values, calculated as in Fig. 1, are: RGS16 = 7 ± 1 nM, RGS16-ILS = 10 ± 1 nM. (B) Dose response curves of RGS16-N (RGS16 K173N) and RGS16-HR + N (RGS16 E164H + K165R + K173N). $EC_{50}$ values are: RGS16-N = 7 ± 1 nM, RGS16-HR + N = 13 ± 1 nM. RGS16 (as in A) is shown for reference. (C) Dose response curves of the RGS16-ILS + HR + N mutant, with RGS16 (as in A), RGS16-ILS (as in A), and RGS16-HR + N (as in B) shown for reference. $EC_{50}$ of RGS16-ILS + HR + N = 17 ± 2 nM. (D) Dose response curves of RGS17 and the RGS16-S* (RGS16 N131S) mutant with RGS16 shown for reference (as in A). $EC_{50}$ values are: RGS17 = 30 ± 2 nM and RGS16-S* = 380 ± 60 nM. Data are means ± SEM of experiments performed in triplicate, representative of three or more independent biological replicates for each RGS.

members with specific Gα subunits by inserting redesigned mutants, such as those presented in this work, into relevant cells and tissues.

## Author contributions

D.S-M. designed the research, conducted most of the experiments and structural analysis, analyzed results, and wrote the paper. A.A. conducted structural analysis and some experiments and analyzed results. M.A-S. conducted experiments, supervised lab work, and analyzed results. M.K. designed and supervised the research and wrote the paper. All authors were involved in the writing of the paper and approved the final version.

## Funding

This work was supported by Israel Science Foundation grants: 1454/13, 1959/13, 2155/15.

## Acknowledgements

We thank Liza Barki-Harrington for helpful comments and acknowledge the contribution of COST Action CM-1207 (GLISTEN) to this work.

## Appendix A. Supplementary data

Supplementary data related to this article can be found at https://doi.org/10.1016/j.bbrc.2018.08.033.

## Transparency document

Transparency document related to this article can be found online at https://doi.org/10.1016/j.bbrc.2018.08.033.

## References

[1] E.M. Ross, T.M. Wilkie, GTPase-activating proteins for heterotrimeric G proteins: regulators of G protein signaling (RGS) and RGS-like proteins, Annu. Rev. Biochem. 69 (2000) 795–827.
[2] S. Hollinger, J.R. Hepler, Cellular regulation of RGS proteins: modulators and integrators of G protein signaling, Pharmacol. Rev. 54 (2002) 527–559.
[3] K.L. Neitzel, J.R. Hepler, Cellular mechanisms that determine selective RGS protein regulation of G protein-coupled receptor signaling, Semin. Cell Dev. Biol. 17 (2006) 383–389.
[4] J.H. Hurst, S.B. Hooks, Regulator of G-protein signaling (RGS) proteins in cancer biology, Biochem. Pharmacol. 78 (2009) 1289–1297.
[5] R.R. Neubig, D.P. Siderovski, Regulators of G-protein signalling as new central nervous system drug targets, Nat. Rev. Drug Discov. 1 (2002) 187–197.
[6] B. Sjogren, L.L. Blazer, R.R. Neubig, Regulators of G protein signaling proteins as targets for drug discovery, Prog. Mol. Biol. Transl. Sci. 91 (2010) 81–119.
[7] A.J. Kimple, D.E. Bosch, P.M. Giguere, D.P. Siderovski, Regulators of G-protein signaling and their G alpha substrates: promises and challenges in their use as drug discovery targets, Pharmacol. Rev. 63 (2011) 728–749.
[8] L. De Vries, M. Mousli, A. Wurmser, M.G. Farquhar, GAIP, a protein that specifically interacts with the trimeric G protein G alpha i3, is a member of a protein family with a highly conserved core domain, Proc. Natl. Acad. Sci. U. S. A. 92 (1995) 11916–11920.
[9] Y. Tu, J. Wang, E.M. Ross, Inhibition of brain Gz GAP and other RGS proteins by palmitoylation of G protein alpha subunits, Science 278 (1997) 1132–1135.
[10] H. Mao, Q. Zhao, M. Daigle, M.H. Ghahremani, P. Chidiac, P.R. Albert, RGS17/RGSZ2, a novel regulator of Gi/o, Gz, and Gq signaling, J. Biol. Chem. 279

(2004) 26314–26322.
[11] C. Nunn, H. Mao, P. Chidiac, P.R. Albert, RGS17/RGSZ2 and the RZ/A family of regulators of G-protein signaling, Semin. Cell Dev. Biol. 17 (2006) 390–399.
[12] M.A. James, Y. Lu, Y. Liu, H.G. Vikis, M. You, RGS17, an overexpressed gene in human lung and prostate cancer, induces tumor cell proliferation through the cyclic AMP-PKA-CREB pathway, Canc. Res. 69 (2009) 2108–2116.
[13] E. Sokolov, D.A. Iannitti, L.W. Schrum, I.H. McKillop, Altered expression and function of regulator of G-protein signaling-17 (RGS17) in hepatocellular carcinoma, Cell. Signal. 23 (2011) 1603–1610.
[14] P. Sanchez-Blazquez, M. Rodriguez-Munoz, C. Bailon, J. Garzon, GPCRs promote the release of zinc ions mediated by nNOS/NO and the redox transducer RGSZ2 protein, Antioxidants Redox Signal. 17 (2012) 1163–1177.
[15] C.R. Bodle, D.I. Mackie, D.L. Roman, RGS17: an emerging therapeutic target for lung and prostate cancers, Future Med. Chem. 5 (2013) 995–1007.
[16] J.L. Glick, T.E. Meigs, A. Miron, P.J. Casey, RGSZ1, a Gz-selective regulator of G protein signaling whose action is sensitive to the phosphorylation state of Gz alpha, J. Biol. Chem. 273 (1998) 26008–26013.
[17] J. Wang, A. Ducret, Y. Tu, T. Kozasa, R. Aebersold, E.M. Ross, RGSZ1, a Gz-selective RGS protein in brain. Structure, membrane association, regulation by G alpha z phosphorylation, and relationship to a Gz GTPase-activating protein subfamily, J. Biol. Chem. 273 (1998) 26014–26025.
[18] Y. Wang, G. Ho, J.J. Zhang, B. Nieuwenhuijsen, W. Edris, P.K. Chanda, K.H. Young, Regulator of G protein signaling Z1 (RGSZ1) interacts with G alpha i subunits and regulates G alpha i-mediated cell signaling, J. Biol. Chem. 277 (2002) 48325–48332.
[19] J.J. Tesmer, D.M. Berman, A.G. Gilman, S.R. Sprang, Structure of RGS4 bound to $AlF4^-$-activated Gi alpha 1: stabilization of the transition state for GTP hydrolysis, Cell 89 (1997) 251–261.
[20] M. Kosloff, A.M. Travis, D.E. Bosch, D.P. Siderovski, V.Y. Arshavsky, Integrating energy calculations with functional assays to decipher the specificity of G protein-RGS protein interactions, Nat. Struct. Mol. Biol. 18 (2011) 846–853.
[21] A. Asli, I. Sadiya, M. Avital-Shacham, M. Kosloff, "Disruptor" residues in the regulator of G protein signaling (RGS) R12 subfamily attenuate the inactivation of G alpha subunits, Sci. Signal. 11 (2018).
[22] M. Soundararajan, F.S. Willard, A.J. Kimple, A.P. Turnbull, L.J. Ball, G.A. Schoch, C. Gileadi, O.Y. Fedorov, E.F. Dowler, V.A. Higman, S.Q. Hutsell, M. Sundstrom, D.A. Doyle, D.P. Siderovski, Structural diversity in the RGS domain and its interaction with heterotrimeric G protein alpha-subunits, Proc. Natl. Acad. Sci. U. S. A. 105 (2008) 6457–6462.
[23] D. Petrey, Z. Xiang, C.L. Tang, L. Xie, M. Gimpelev, T. Mitros, C.S. Soto, S. Goldsmith-Fischman, A. Kernytsky, A. Schlessinger, I.Y. Koh, E. Alexov, B. Honig, Using multiple structure alignments, fast model building, and energetic analysis in fold recognition and homology modeling, Proteins 53 (Suppl 6) (2003) 430–435.
[24] Z. Xiang, B. Honig, Extending the accuracy limits of prediction for side-chain conformations, J. Mol. Biol. 311 (2001) 421–430.
[25] M. Natochin, R.L. McEntaffer, N.O. Artemyev, Mutational analysis of the Asn residue essential for RGS protein binding to G-proteins, J. Biol. Chem. 273 (1998) 6731–6735.
[26] B.A. Posner, S. Mukhopadhyay, J.J. Tesmer, A.G. Gilman, E.M. Ross, Modulation of the affinity and selectivity of RGS protein interaction with G alpha subunits by a conserved asparagine/serine residue, Biochemistry 38 (1999) 7773–7779.
[27] K.C. Slep, M.A. Kercher, T. Wieland, C.K. Chen, M.I. Simon, P.B. Sigler, Molecular architecture of G alpha o and the structural basis for RGS16-mediated deactivation, Proc. Natl. Acad. Sci. U. S. A. 105 (2008) 6243–6248.
[28] M. Kasom, S. Gharra, I. Sadiya, M. Avital-Shacham, M. Kosloff, Interplay between negative and positive design elements in G alpha helical domains of G proteins determines interaction specificity towards RGS2, Biochem. J. 475 (14) (2018) 2293–2304.
[29] M. Kosloff, Z. Selinger, GTPase catalysis by Ras and other G-proteins: insights from substrate directed superimposition, J. Mol. Biol. 331 (2003) 1157–1170.
[30] S.P. Srinivasa, N. Watson, M.C. Overton, K.J. Blumer, Mechanism of RGS4, a GTPase-activating protein for G protein alpha subunits, J. Biol. Chem. 273 (1998) 1529–1533.

## Supplementary material

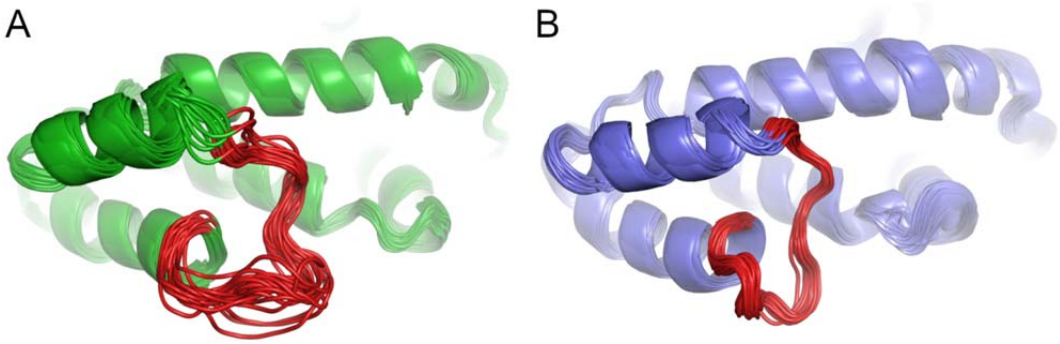


Figure S1: The RZ subfamily representative RGS19 shows ehnaced flexibility in the α5-α6 loop compared to the R4 respresentative RGS4. (A) The 20 NMR models of the RGS19 monomer structure (PDB ID 1CMZ, green ribbon) show enhanced conformational variability in the α5-α6 loop, which contains the ILS motif. (B) The 30 NMR models of monomeric RGS4 (PDB ID 1EZY, blue ribbon) show that the α5-α6 loop has a fixed rigid structure among all models. The structures are shown as ribbon diagram with the α5-α6 loop colored red.

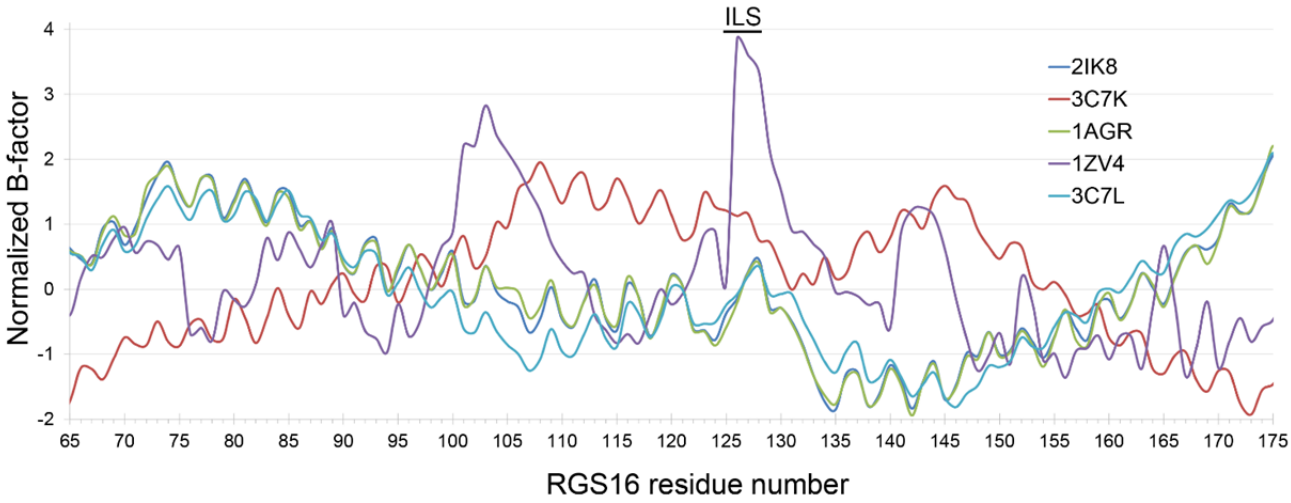


Figure S2: The RGS17 ILS motif has higher thermal B-factors than the corresponding residues in representative R4 subfamily crystal structures. Plotted are normalized thermal B-factors for the RGS domains from the following structures (with PDB IDs): RGS16-$G\alpha_{i1}$ (2IK8), RGS16-$G\alpha_{o}$ (3C7K), RGS4-$G\alpha_{i1}$ (1AGR), RGS17 (1ZV4), and RGS16 (3C7L).